The Astrophysical Journal, 628:938–945, 2005 August 1
© 2005. The American Astronomical Society. All rights reserved. Printed in U.S.A.

AN *XMM-NEWTON* VIEW OF THE SOFT GAMMA REPEATER SGR 1806−20: LONG-TERM VARIABILITY IN THE PRE–GIANT FLARE EPOCH[1]

S. Mereghetti, A. Tiengo,[2] P. Esposito,[2] and D. Götz
INAF—Istituto di Astrofisica Spaziale e Fisica Cosmica, Sezione di Milano "G.Occhialini," v. Bassini 15, I-20133 Milan, Italy

L. Stella, G. L. Israel, and N. Rea[3]
INAF—Osservatorio Astronomico di Roma, via Frascati 33, I-00040 Monteporzio Catone, Italy

M. Feroci
INAF—Istituto di Astrofisica Spaziale e Fisica Cosmica, Sezione di Roma, v. Fosso del Cavaliere 100, I-00133 Rome, Italy

R. Turolla
Universitá di Padova, Dipartimento di Fisica, via Marzolo 8, I-35131 Padua, Italy

and

S. Zane
Mullard Space Science Laboratory, University College London, Holmbury St. Mary, Dorking Surrey, RH5 6NT, UK
Received 2005 January 29; accepted 2005 April 12

ABSTRACT

The low-energy (<10 keV) X-ray emission of the soft gamma repeater SGR 1806−20 has been studied by means of four *XMM-Newton* observations carried out in the last two years, the latest performed in response to a strong sequence of hard X-ray bursts observed on 2004 October 5. The source was caught in different states of activity; over the 2003–2004 period, the 2–10 keV flux doubled with respect to the historical level observed previously. The long-term rise in luminosity was accompanied by a gradual hardening of the spectrum, with the power-law photon index decreasing from 2.2 to 1.5, and by a growth of the bursting activity. The pulse period measurements obtained in the four observations are consistent with an average spin-down rate of 5.5×10^{-10} s s^{-1}, higher than the values observed in the previous years. The long-term behavior of SGR 1806−20 exhibits the correlation between spectral hardness and spin-down rate previously found only by comparing the properties of different sources (both SGRs and anomalous X-ray pulsars [AXPs]). The best-quality spectrum (obtained on 2004 September 6) cannot be fitted by a single power law but requires an additional blackbody component [$kT_{\rm BB} = 0.79$ keV, $R_{\rm BB} = 1.9\ (d/15\ {\rm kpc})^2$ km], similar to the spectra observed in other SGRs and AXPs. No spectral lines were found in the persistent emission, with equivalent width upper limits in the range 30–110 eV. Marginal evidence for an absorption feature at 4.2 keV is present in the cumulative spectrum of 69 bursts detected in 2004 September-October.

Subject headings: stars: individual (SGR 1806−20) — stars: neutron — X-rays: bursts

1. INTRODUCTION

The high-energy sources known as SGRs are probably one of the most intriguing manifestations of young neutron stars. They were first discovered as transient phenomena through the observation of short (<1 s) gamma-ray bursts. The detection of several bursts coming from the same sky directions, coupled with their softer spectra, clearly set them apart from the standard gamma-ray bursts and led to the definition of this small class of sources. Only three confirmed SGRs are known in our Galaxy and one in the Large Magellanic Cloud (LMC; see Hurley 2000 for a review).

The nature of SGR bursts remained a mystery for many years. The 8 s periodicity seen during an exceptionally bright flare from the LMC SGR 0525−66 (Mazets et al. 1979), as well as the spatial coincidence of this SGR with the supernova remnant N49 (Cline et al. 1982), suggested that neutron stars could be involved in SGRs, but a confirmation had to wait for the discovery of their persistent counterparts in the classical X-ray range (<10 keV). At these energies SGRs are generally observed as pulsating sources with periods of several seconds, secular spin-down in the range $\sim10^{-11}$ to 10^{-10} s s^{-1}, and X-ray luminosity orders of magnitude larger than their rotational energy loss (see, e.g., Woods & Thompson 2004 for a recent review).

The SGR properties are successfully explained by the "magnetar" model (Duncan & Thompson 1992; Thompson & Duncan 1995). Magnetars are neutron stars in which the dominant source of free energy is a very intense magnetic field ($B \sim 10^{14}$–10^{15} G), rather than rotation as in ordinary radio pulsars. Such a high magnetic field can be produced by an efficient dynamo mechanism that operates if the neutron star is born with a very short (~1 ms) period (Thompson & Duncan 1993). In the magnetar model the short bursts are produced by small cracks in the neutron star crust, driven by the magnetic field diffusion (Thompson & Duncan 1995), or, alternatively, by the sudden loss of magnetic equilibrium, through the development of a tearing instability (Lyutikov 2002, 2003). The much more energetic flares sporadically seen in SGRs are the result of global reconfigurations of the neutron star magnetosphere.

In this work we concentrate on SGR 1806−20, the most prolific SGR, which showed several periods of bursting activity since the time of its discovery in 1979 (Laros et al. 1986). Its

[1] Based on observations obtained with *XMM-Newton*, an ESA science mission with instruments and contributions directly funded by ESA Member States and NASA.

[2] Università degli Studi di Milano, Dipartimento di Fisica, via Celoria 16, I-20133 Milan, Italy.

[3] SRON—National Institute for Space Research, Sorbonnelaan, 2, 3584 CA, Utrecht, Netherlands.

TABLE 1
JOURNAL OF *XMM-Newton* OBSERVATIONS AND TIMING RESULTS

OBSERVATION	DATE	DURATION (ks)	MODE[a] AND EXPOSURE TIME		PULSE PERIOD (s)
			pn Camera	MOS Cameras	
A	2003 Apr 03	30	FF (5.4 ks)	LW (6 ks)	7.5311 ± 0.0003
B	2003 Oct 07	22	FF (13.4 ks)	LW (17 ks)	7.5400 ± 0.0003
C	2004 Sep 06	52	SW (36.0 ks)	LW (51 ks)	7.55592 ± 0.00005
D	2004 Oct 06	19	SW (12.9 ks)	Ti (18 ks)	7.5570 ± 0.0003

[a] FF = Full Frame (time resolution 73 ms); LW = Large Window (time resolution 0.9 s); SW = Small Window (time resolution 6 ms); Ti = Timing (time resolution 1.5 ms).

persistent X-ray counterpart was discovered with the *ASCA* satellite (Murakami et al. 1994) and studied in more detail with *RXTE* and *BeppoSAX*. The *RXTE* observations led to the discovery of pulsations (period $P = 7.47$ s and period derivative $\dot{P} = 8 \times 10^{-11}$ s s^{-1}; Kouveliotou et al. 1998) and were subsequently used to study in detail the timing properties of the source, such as the long-term $\dot{P}$ variations (Woods et al. 2000, 2002) and the evolution of the pulse profile (Göğüş et al. 2002). The best X-ray spectra reported to date were obtained by *BeppoSAX* in 1998 October and 1999 March (Mereghetti et al. 2000). These showed a spectrum equally well described in the 2–10 keV range by a power law with photon index $\Gamma = 1.95$ or by a thermal bremsstrahlung with temperature $kT_{\rm tb} = 11$ keV. Similar flux values were measured by all the above satellites, indicating a fairly stable luminosity of $\sim 3 \times 10^{35}$ $(d/15\ {\rm kpc})^2$ ergs s^{-1} (2–10 keV) in the period 1993–2001. Thanks to the unprecedented imaging capabilities of the *INTEGRAL* satellite in the hard X-ray/soft γ-ray range, the study of the persistent emission from SGRs has been recently extended to higher energies; observations of SGR 1806−20 carried out in 2003–2004 showed a power-law spectrum with photon index $\Gamma \sim 1.5$–1.9 extending up to 150 keV (Mereghetti et al. 2005a; Molkov et al. 2005).

During the last 2 years SGR 1806−20 displayed a gradual increase in the level of activity, as testified by the rate at which bursts were emitted and by an increase of the soft and hard X-ray luminosity (Woods et al. 2004; Mereghetti et al. 2005a), which culminated on 2004 December 27 with the emission of the first giant flare seen from this source (Borkowski et al. 2004; Mazets et al. 2004).

Here we report on a series of *XMM-Newton* observations of SGR 1806−20, obtained from 2003 April to 2004 October, which show a similar pattern of long-term increasing activity also in the classical X-ray range: while in 2003 the 2–10 keV emission was similar to that seen in previous measurements with other satellites, the source flux doubled in the following year. These observations allowed us to study with unprecedented detail the properties of the persistent emission below 10 keV, by means of phase-averaged and phase-resolved spectroscopy, and also to obtain some information on the average spectral properties of a sample of bursts.

2. OBSERVATIONS AND DATA REDUCTION

A summary of all the *XMM-Newton* observations of SGR 1806−20 reported here is given in Table 1. We used data obtained with the EPIC instrument consisting of two MOS and one pn cameras (Turner et al. 2001; Strüder et al. 2001). The first observation (2003 April) was strongly affected by high particle background, resulting in a usable time of only ∼5 ks. Although SGR 1806−20 was in an apparently quiescent state, one burst could be identified through a careful analysis of the light curve. The next observation (2003 October) had a longer exposure, but no bursts were detected, despite the source being in a fairly active period; bursts were detected by *INTEGRAL* the day before and after the *XMM-Newton* observation (Mereghetti et al. 2003).

In 2004 September, SGR 1806−20 was observed again for ∼50 ks while it was in an active state. This is the observation providing the highest quality data; no strong background flares were present, and the source count rate was about a factor of 2 higher than in the previous observations. Since the likely detection of bursts was anticipated, the pn camera was set in Small Window mode in order to reduce pile-up effects at burst peaks. In fact, about 40 bursts were detected. Finally, a Target of Opportunity observation was obtained following an unusual sequence of clustered soft bursts detected by *INTEGRAL* and Konus on October 5 (Mereghetti et al. 2004; Golenetski et al. 2004). Again, about 30 bursts were detected. The MOS was in Timing mode, which provides a time resolution of 1.5 ms at the expense of imaging only along a single direction.

In all the observations the medium thickness filter was used. All the data reduction was performed using the *XMM-Newton* Science Analysis Software (SAS ver. 6.0.0). The raw observation data files were processed using standard pipeline tasks (`epproc` for pn, `emproc` for MOS data).

3. SPECTRAL ANALYSIS

The source spectra were extracted from circular regions centered at the position of SGR 1806−20. For the last two observations (C and D) a radius of 40″ was chosen, while for observations A and B, which have a higher particle background even after filtering out the main proton flares, a smaller radius of 25″ was preferred in order to increase the signal-to-noise ratio. The background spectra were extracted from a region of the same chip as the source, far enough to avoid significant contamination by its photons. We selected events with pattern 0–4 and pattern 0–12 for the pn and the MOS, respectively. The source spectra were rebinned in order to have at least 30 counts per energy bin while avoiding oversampling of the instrumental energy resolution. We limited the spectral analysis to the 1.5–12 keV range, since, due to the high interstellar absorption (SGR 1806−20 lies in the Galactic plane, at only 10° from the Galactic center direction), very few source counts are detected at lower energies.

We concentrate first on the pn spectra of the 2004 September observation (observation C). This is the data set with the best statistical quality, owing to the high source count rate and long observing time. A fit with an absorbed power law yields a relatively high χ^2 value ($\chi^2_{\rm red} = 1.37$) and structured residuals, while a much better fit ($\chi^2_{\rm red} = 0.93$) can be obtained by adding a blackbody component. The best-fit spectrum is illustrated in Figure 1. The best-fit parameters are photon index $\Gamma = 1.2$,

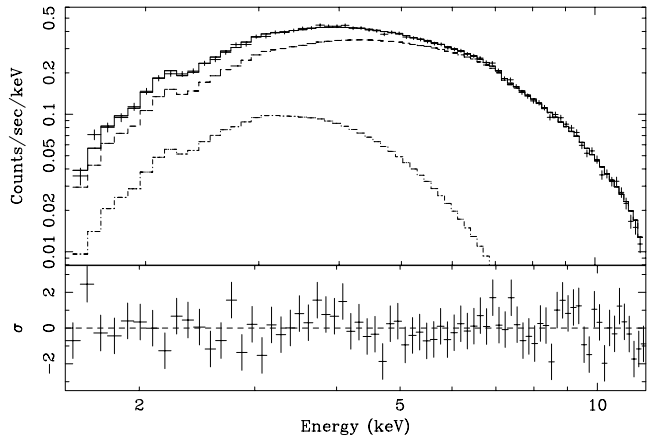


FIG. 1.—EPIC pn spectrum of SGR 1806−20 for the observation of 2004 September 6 (obs. C). *Top*: Data and best-fit model (*solid line*). The two spectral components, power law and blackbody (*lower curve*), are indicated by the dashed lines. *Bottom*: Residuals from the best-fit model in units of σ.

blackbody temperature $kT_{\rm BB} = 0.79$ keV, and absorption $N_{\rm H} \sim 6.5\times10^{22}$ cm^{-2}. We have verified that the presence of bursts, which contribute to less than 1% of the total source counts, has a negligible effect on the source spectrum.

In Table 2 we compare, for the four observations, the results obtained using either a power law or a power-law plus blackbody model. Although not formally required in observations A, B, and D, which are reasonably well fitted by single power laws, the presence of the additional blackbody component is consistent with all the spectra and yields χ^2 values systematically lower than the single power-law fits. Except for the flux, which increased from $\sim1.2\times10^{-11}$ ergs cm^{-2} s^{-1} of observation A to $\sim2.4\times10^{-11}$ ergs cm^{-2} s^{-1} of observations C and D, all the other spectral parameters are, within the errors, consistent with constant values. We therefore explored the possibility of describing the data by forcing some of the parameters to common values for all the observations. This was done by jointly fitting the four data sets and resulted in best-fit values of $\Gamma = 1.36$, $kT_{\rm BB} = 0.65$ keV, and a blackbody emitting area of 18 km^2 for an assumed distance of 15 kpc (Corbel & Eikenberry 2004). The variations can be reproduced by changing only the normalization of the power-law component. We also analyzed in a similar way the spectra obtained with the MOS cameras, obtaining results consistent with the pn ones.

TABLE 3

UPPER LIMITS (AT 3 σ) ON SPECTRAL FEATURES IN THE pn SPECTRA OF SGR 1806−20 FROM OBSERVATION C

Energy Range (keV)	σ (eV)	Equivalent Width (eV)
2–3	0	<28
	100	<65
	200	<100
3–7	0	<22
	100	<32
	200	<55
7–10	0	<55
	100	<70
	200	<110

No evidence for spectral lines, in emission or in absorption, was found by looking at the residuals from the best-fit models. We computed upper limits on the lines' equivalent widths as a function of the assumed line energy and width. This was done by adding Gaussian components to the model and computing the allowed range in their normalization. The most stringent results, obtained from the pn data of observation C, are summarized in Table 3.

4. TIMING ANALYSIS AND PHASE-RESOLVED SPECTROSCOPY

For the timing analysis we first corrected the time of arrival of the source events to the solar system barycenter and then used standard folding and phase-fitting techniques to measure the source spin period. Pulsations were clearly detected in all the observations, with the period values given in Table 1. A linear fit to the four *XMM-Newton* period measurements gave a spin-down of $\dot{P} = (5.49 \pm 0.09)\times10^{-10}$ s s^{-1}.

In Figure 2 we show the background-subtracted light curves in different energy ranges for the four observations. Their shape, characterized by a relatively large duty cycle, is quite similar to that observed with *RXTE* (Göğüş et al. 2002). To derive the pulsed fractions we fitted a sinusoid plus a constant to the background-subtracted light curves. The pulsed fractions, defined

TABLE 2

SUMMARY OF THE SPECTRAL RESULTS

Observation	Absorption (10^{22} cm^{-2})	Power-Law Photon Index	$kT_{\rm BB}$ (keV)	$R_{\rm BB}$[a] (km)	PL Flux[b] (10^{-11} ergs cm^{-2} s^{-1})	$\chi^2_{\rm red}$ (dof)
A	6.31 (5.88–6.78)	1.63 (1.52–1.75)	...	...	1.226 (1.216–1.233)	1.03 (58)
B	6.10 (5.83–6.38)	1.55 (1.48–1.62)	...	...	1.379 (1.374–1.384)	1.11 (70)
C	6.69 (6.56–6.82)	1.51 (1.48–1.54)	...	...	2.651 (2.645–2.656)	1.37 (72)
D	6.70 (6.50–6.91)	1.57 (1.52–1.62)	...	...	2.670 (2.664–2.676)	1.13 (71)
A	6.64 (5.62–8.40)	1.44 (1.03–1.70)	0.59 (0.44–0.91)	2.6 (0.7–13.9)	1.16 (1.01–1.23)	1.01 (56)
B	6.05 (4.92–6.64)	1.20 (0.49–1.40)	0.73 (0.57–0.99)	1.8 (1.2–2.9)	1.25 (1.01–1.39)	0.97 (68)
C	6.51 (6.24–6.88)	1.21 (1.09–1.35)	0.79 (0.67–0.88)	1.9 (1.6–2.6)	2.42 (2.32–2.52)	0.93 (70)
D	6.53 (5.92–7.10)	1.23 (0.90–1.42)	0.77 (0.61–0.94)	2.2 (1.6–3.5)	2.41 (2.12–2.70)	0.90 (69)
A	6.78 (6.56–6.98)	1.36 (1.31–1.41)	0.65 (0.59–0.72)	2.4 (1.9–3.1)	1.11 (1.08–1.24)	0.98 (57)
B	6.78 (6.56–6.98)	1.36 (1.31–1.41)	0.65 (0.59–0.72)	2.4 (1.9–3.1)	1.26 (1.23–1.38)	0.98 (66)
C	6.78 (6.56–6.98)	1.36 (1.31–1.41)	0.65 (0.59–0.72)	2.4 (1.9–3.1)	2.54 (2.51–2.65)	0.97 (68)
D	6.78 (6.56–6.98)	1.36 (1.31–1.41)	0.65 (0.59–0.72)	2.4 (1.9–3.1)	2.59 (2.56–2.70)	1.06 (67)

NOTE.—Errors are at the 90% c.l. for a single interesting parameter.

[a] Radius at infinity assuming a distance of 15 kpc.

[b] Absorbed flux of the power-law component as observed by the pn in the 2–10 keV energy range.

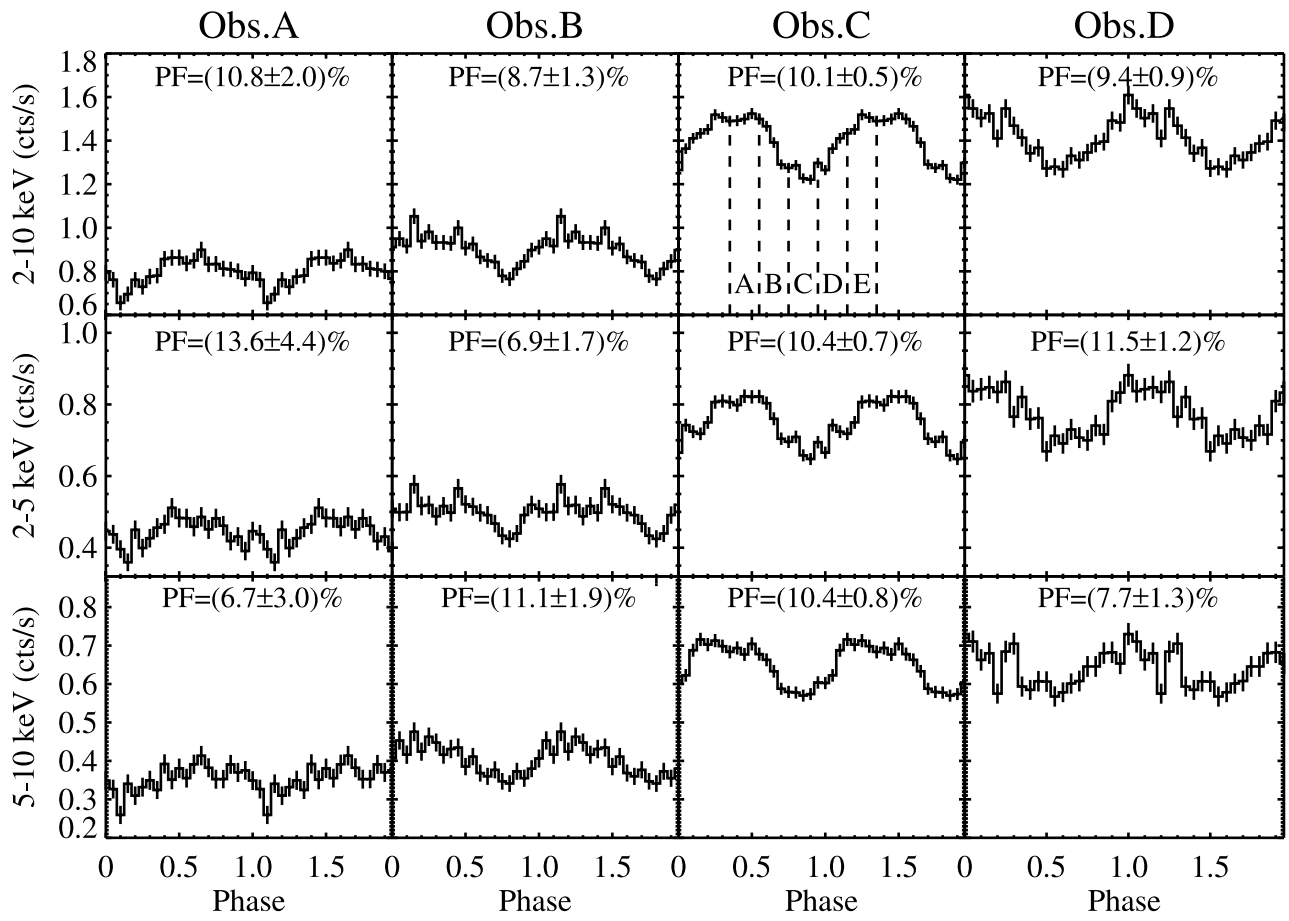


FIG. 2.—Folded light curves in the total (2–10 keV), soft (2–5 keV), and hard (5–10 keV) energy range for the four observations. The background has been subtracted. The pulsed fraction is indicated on each panel (1 σ errors). The vertical lines in obs. C indicates the phase intervals used for the phase-resolved spectroscopy.

as the amplitude of the sinusoid divided by the constant, are in the ~6%–14% range (the values are reported in the corresponding panels of Fig. 2).

To assess the statistical significance of possible pulse shape variations as a function of time and/or energy range, we compared the folded light curves using a Kolmogorov-Smirnov test. The results show that the difference between the soft and hard energy range during observation C is highly significant (the probability that the two profiles come from the same underlying distribution is $\sim 10^{-4}$). The corresponding value for observation D is much higher, 0.01, but still indicates a possible difference between the two energy ranges. On the other hand the differences between the four observations are not significant (all the probabilities are larger than 10%).

During observation C enough source photons were collected to perform a meaningful phase-resolved spectroscopy. We extracted five spectra from the phase intervals shown in Figure 2, following the same method used for the average spectra. No significant spectral variations with phase were detected, all these spectra being consistent with the model and parameters of the phase-averaged spectrum, simply rescaled by an overall normalization factor. It is interesting to note that a fit of comparable statistical quality is obtained if the power-law normalization instead of the total flux is allowed to be the only phase-dependent parameter. This suggests the possibility that the blackbody component is stable and the variations with the pulsation phase are due entirely to the power-law component.

Finally, the search for possible spectral lines was also extended to the phase-resolved spectra, again with negative results. The upper limits on the equivalent widths are typically a factor of ~3 larger than the corresponding values reported in Table 3 for the phase-averaged spectrum.

5. ANALYSIS OF THE BURSTS

Visual inspection of the light curves binned at 0.1 s clearly showed the presence of tens of bursts in observations C and D. For the other two observations the search for bursts was hampered by the higher background level and the worse time resolution of the pn in full-frame mode, and only a single burst in observation A could be identified. The light curves of some of the brightest bursts detected during observation D are shown in Figure 3.

Individual bursts have too few counts for a meaningful spectral analysis. Therefore, we extracted a cumulative spectrum of all the bursts detected during observations C and D using counts from the entire pn Small Window (only the window borders have been masked). This corresponds to a total exposure of 12.7 s and contains about 2000 net counts in the 2–10 keV range. The spectrum of the remaining observing time was used as background.

Fits with simple models (power law, thermal bremsstrahlung, and blackbody) all give formally acceptable χ^2 values. The power law and the bremsstrahlung require a large absorption ($N_{\rm H} = 10^{23}$ cm^{-2}), and the bremsstrahlung temperature is not well constrained. We therefore favor the blackbody model, which yields an absorption value consistent with that of the persistent emission. The best-fit parameters are $kT_{\rm BB} = 2.3 \pm 0.2$ keV and $N_{\rm H} = (6 \pm 1) \times 10^{22}$ cm^{-2} (see Fig. 4). The residuals from this

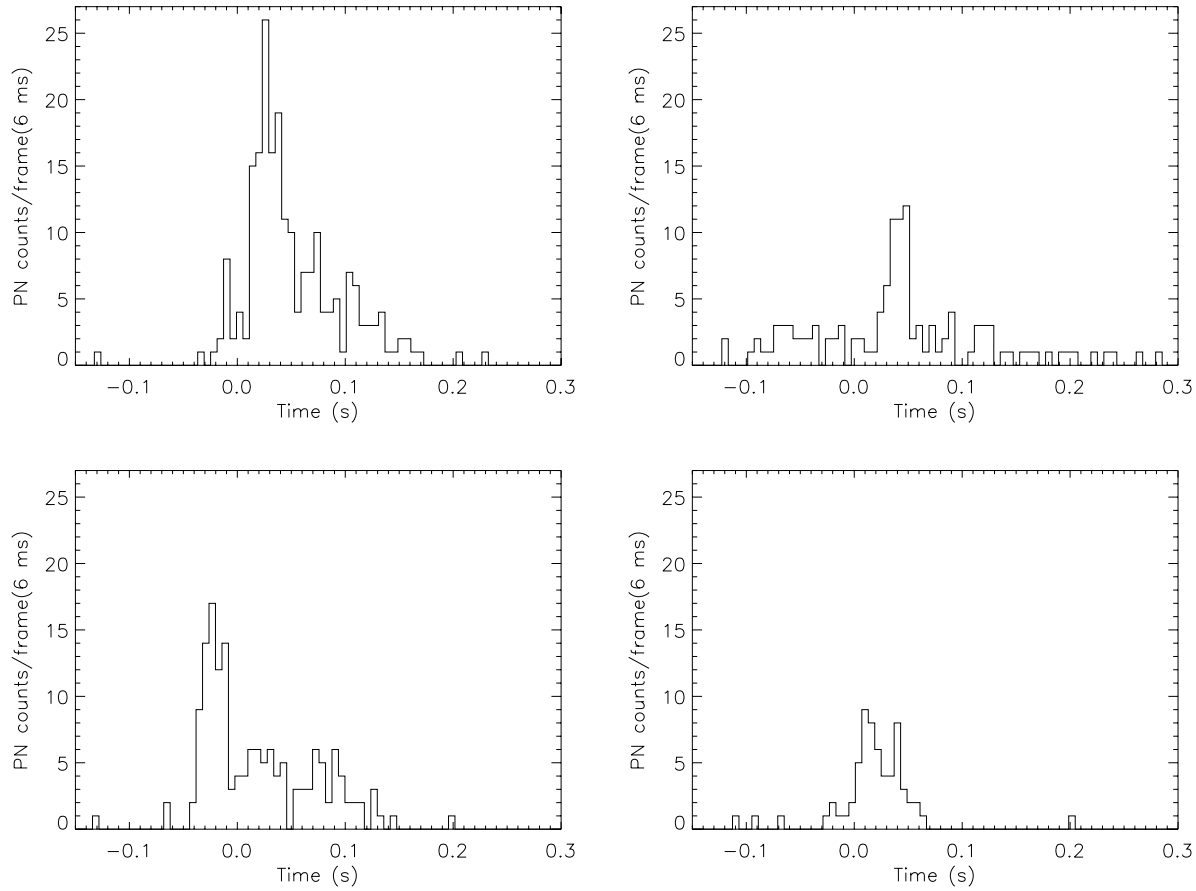


FIG. 3.—Light curves of four bursts detected during obs. D. Less than 0.02 background events per frame are expected.

best fit show a deviation at 3.3 σ, at 4.2 keV. This feature could not be reproduced in other spectra obtained with different data selections and binning criteria. Therefore, we consider it to be only marginal evidence of an absorption line. Note that the absorption features previously reported in some bursts from this source were at a slightly different energy of $\sim$5 keV (Ibrahim et al. 2003).

For a few bursts included in the above analysis the large count rate at the peak can produce photon pile-up. An exact estimate of this effect and its correction are difficult to obtain in this case, owing to the rapid variability during bursts. To verify the robustness of our spectral results we tried different data selection aimed at reducing the fraction of piled-up events. We found that the shape of the spectrum does not change significantly by either removing the photons of the brightest (parts of the) bursts,[4] or using an annular extraction region, or taking only events with pattern 0 (single pixel). In conclusion we estimate that our analysis of the cumulative spectrum gives a reasonable indication of the average spectral shape of the bursts.

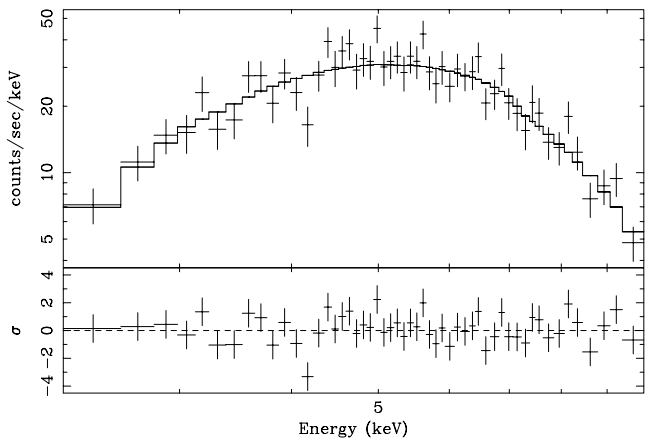


FIG. 4.—EPIC pn spectrum of the sum of 69 bursts detected in obs. C and D. *Top*: Data and best-fit model with a blackbody of temperature $kT = 2.3$ keV. *Bottom*: Residuals from the best-fit model in units of σ.

6. BROADBAND SPECTROSCOPY WITH *XMM-NEWTON* AND *INTEGRAL*

The *INTEGRAL* observations of SGR 1806−20 (Mereghetti et al. 2005a) can in principle be used together with the *XMM-Newton* data to study the source spectrum over the broad 1–150 keV energy range. Although the conclusions of this analysis are dependent on the current uncertainties in the relative calibration of the two satellites, we report here the results for future reference and as a possible contribution to assess this issue.

We have considered the *INTEGRAL* spectra accumulated during three periods[5] that overlap the *XMM-Newton* data: 2003 March 12–April 23, 2003 September 27–October 15, and 2004 September 21–October 14. These spectra, obtained with the IBIS instrument (Ubertini et al. 2003) and analyzed as described in Mereghetti et al. (2005a), have been fitted together with those

[4] The best-fit blackbody model excluding data with more than 20 counts per frame gives $kT_{\rm BB} = 2.32 \pm 0.23$ keV and $N_{\rm H} = (6.0 \pm 1.3) \times 10^{22}$ cm^{-2}.

[5] Since long exposure times are required to detect the source in the hard X-ray range, it is not possible to restrict the analysis to the *INTEGRAL* data strictly simultaneous with the *XMM-Newton* observations.

of the EPIC pn. The joint fits are consistent with the parameters derived only with *XMM-Newton* (Table 2) if the IBIS data in the 20–150 keV are scaled upward by a factor of ∼1.3 or ∼2 in the PL or PL+BB case, respectively. Alternatively, a spectral steepening above the EPIC range is required. For example, good fits are obtained with a photon index $\Gamma = 1.8$ above 12 keV.

7. DISCUSSION

Our last observation (observation D) was carried out as a Target of Opportunity in order to study possible variations in the source properties related to the strong bursting activity seen at high energies (>20 keV) on 2004 October 5, when two clusters of powerful bursts were emitted in a time span of a few minutes (Mereghetti et al. 2004). The individual events had spectra and duration similar to those of the normal bursts, but they had rather high peak fluxes and were grouped in a way never observed before in this source, yielding a total fluence of $\sim 10^{-4}$ ergs cm^{-2} (Golenetskii et al. 2004). The *XMM-Newton* observation, which started only 27 hr after this energetic event, did not show particularly striking changes in the source spectrum and pulse profile. There is some evidence of a more structured pulse profile above 5 keV, but the statistical significance is not compelling. This means that the October 5 event did not cause changes in the mechanisms responsible for the persistent emission and in magnetic field configuration that were strong and/or long-lasting enough to affect the source properties significantly after ∼1 day.

Thanks to the high statistics in the spectrum of the persistent emission obtained in 2004 September (observation C), we could set stringent limits on the presence of lines and found evidence for an additional blackbody component with temperature $kT_{\rm BB} \sim 0.8$ keV. This component was not required in the spectra from the previous observations, when the source had a lower luminosity, but the data are consistent with it being always present with a constant temperature and emitting area. A similar thermal component, albeit with a lower temperature, was also reported in *Chandra* observations of SGR 1806−20 performed in 2004 May–June (Woods et al. 2004). During these observations, the source soft X-ray flux was already larger than the "historical" level of $\sim 1.3 \times 10^{-11}$ ergs cm^{-2} s^{-1}. A blackbody component has also been observed in the other well-studied soft repeater SGR 1900+14 (Woods et al. 2001), where it was more prominent when the source was in a relatively quiescent state. The two-component spectrum reinforces the similarity between SGRs and anomalous X-ray pulsars, where the two-component model has a ubiquitous character (e.g., Mereghetti et al. 2002a), and which are also believed to be magnetars.

The power-law photon indices[6] of SGR 1806−20 obtained in the four *XMM-Newton* observations ($\Gamma \sim 1.5$) are significantly smaller than those observed in 1993 with *ASCA* ($\Gamma = 2.2 \pm 0.2$; Sonobe et al. 1994) and in 1998–2001 with *BeppoSAX* ($\Gamma = 1.97 \pm 0.09$; Mereghetti et al. 2002b). This indicates that a spectral hardening occurred between 2001 September and 2003 April. In this time interval, only *RXTE* observed SGR 1806−20 during a monitoring program mainly focused on the source timing properties, and no spectral results (which could establish when exactly the spectral change occurred) have been reported to date. On the other hand, these *RXTE* observations indicate that the average spin-down rate changed in 2000. While the early sparse period measurements with *ASCA* and *BeppoSAX* (Mereghetti et al. 2002b), as well as a phase-connected *RXTE* timing solution spanning 1999 February–August (Woods et al. 2000), are consistent with an average $\dot{P} \sim 8.5 \times 10^{-11}$ s s^{-1}, subsequent *RXTE* data indicate a spin-down larger by a factor of ∼4 (Woods et al. 2002). Our period measurements show a further increase in the average $\dot{P}$, as shown in Figure 5.

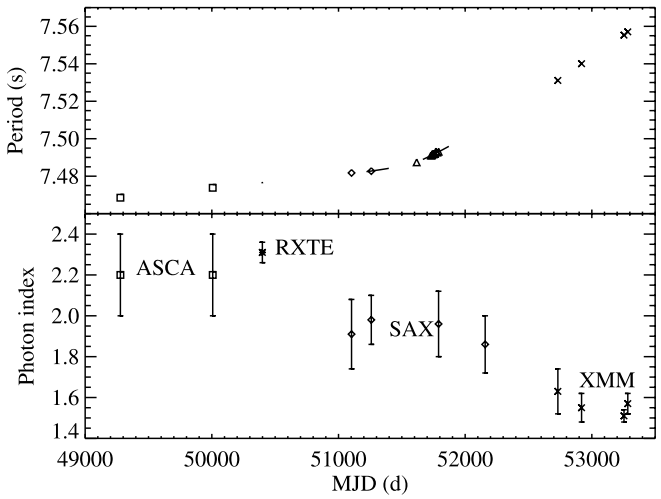


FIG. 5.—Long-term evolution of the pulse period (*top*) and power-law photon index (*bottom*) of SGR 1806−20. To derive the fourth *BeppoSAX* data point in the lower panel, we have analyzed an unpublished observation performed on 2001September 6.

A correlation between spectral hardness and spin-down rate is present in the sample of AXPs and SGRs. The sources with the harder spectrum have a larger long-term spin-down rate (Marsden & White 2001). The results shown in Figure 5 for SGR 1806−20 indicate, for the first time, that such a correlation also holds within different states of a single source.

All the results discussed above are consistent with the magnetar scenario. In particular, the observed long-term variations, the correlation between spectral hardening and spin-down rate, and the increase in the bursting activity fit reasonably well with what is expected in a twisted magnetosphere (see Thompson et al. 2002). In this scenario, SGRs and AXPs differ from standard radio pulsars, since their magnetic field is globally twisted inside the star, up to a strength about 10 times the external dipole, and, at intervals, can twist up the external field. Twisted, force-free magnetospheres ($B_\phi \neq 0$) support currents, and the charges flowing in the magnetosphere may produce a significant optical depth to electron and ion scattering. Since scattering is resonant at the cyclotron frequency ω_B, thermal photons emitted at the star surface scatter at different radii, where $\omega = \omega_B(R)$. In the case of electrons, the charge distribution is spatially extended, and repeated scatterings lead to the formation of a high-energy tail (instead of a narrow line). A gradually increasing twist results in a larger optical depth, and this causes a hardening of the X-ray spectrum.

At the same time, the spin-down rate increases because, for a fixed dipole field, the fraction of field lines that open out across the speed-of-light cylinder grows. Since both the spectral hardening and the spin-down rate increase with the twist, the model predicts that they should be correlated. This trend is actually present in the data reported here (see Fig. 5). According to the magnetar model, the stresses building up in the neutron star crust and the magnetic footprint movements can lead to crustal fractures that can be energetic enough to explain the observed increase in the bursting activity (but see Jones 2003).

[6] Since the previous results were described without the additional blackbody component, we compare the fits with a single power law.

The charges present in the magnetosphere also provide a large optical depth to resonant proton (ions) cyclotron scattering. The proton resonance sits much closer to the star surface than the electron resonance and therefore is less sensitive to the broadening caused by the radial dependence of B. However, this is not sufficient to make spectral lines detectable because, in the general case, positive charges are not confined in a thin layer close to the star surface. This implies that lines in the persistent emission are difficult to observe because the scattering occurs in a region where the magnetic field is varying.

Interestingly, this scenario may provide an explanation for the transient appearance of a cyclotron line as that tentatively detected at 4 keV during the bursts seen with *XMM-Newton* and at 5 keV with *RXTE* (Ibrahim et al. 2002, 2003), at times when the source has a particularly large luminosity and hard spectrum. In fact, when the luminosity at $\omega_B(R_*)$ exceeds the luminosity produced by surface heating by returning currents ($L_X^{rc} \approx 10^{35}$–10^{36} ergs s^{-1}; see eq. [34] of Thompson et al. 2002), protons may accumulate close to the surface owing to the large radiation force. Under these conditions, i.e., the existence of a twisted, current-carrying magnetosphere *and* a large transient flux (above L_X^{rc}) at the cyclotron resonance, the formation of a line may be expected. The persistent luminosity of SGR 1806−20 in the range 4–5 keV is below L_X^{rc}, while the average burst luminosity in the same energy range is $\gtrsim 2 \times 10^{36}$ ergs s^{-1}, much larger than L_X^{rc}. The different energy at which the line has been possibly detected with *XMM-Newton* and *RXTE* may be explained in terms of a variation ($\approx$10%) of the average surface field along the line of sight in the two epochs, which in turn can be due to different twisting properties or quadrupolar components, to which the proton cyclotron line is very sensitive.

Up to now, limited spectral information has been obtained for SGR bursts below 20 keV, in particular with high spectral resolution and good sensitivity at a few keV. Several studies have provided increasing evidence that the optically thin thermal bremsstrahlung model, which gives a good phenomenological description of the SGR burst spectra in the hard X-ray range, is inconsistent with the data below 15 keV (Fenimore et al. 1994; Olive et al. 2004). Recently, Feroci et al. (2004) analyzed a sample of bursts from SGR 1900+14 using *BeppoSAX* data in the 1.5–200 keV range and obtained good fits with a model consisting of two blackbodies with average temperatures of about 3 and 10 keV. Our results are consistent with a similar situation also for SGR 1806−20 and confirm earlier indications in this sense (e.g., Laros et al. 1986).

8. CONCLUSIONS

The *XMM-Newton* monitoring of SGR 1806−20 carried out over the last two years has allowed us to perform a detailed study of its soft X-ray emission, in particular, for what concerns the spectral properties and long-term variability. Our results are particularly interesting when compared to earlier *ASCA* and *BeppoSAX* measurements and put in the broader context of observations at higher energies. The emerging scenario is that of long-term growth in the level of nonthermal magnetospherical activity, finally leading to the exceptional event observed on 2004 December 27.

More specifically, we found that

1. A single power law is inadequate to fit the 2–10 keV spectrum with the highest statistical quality; an additional blackbody component, too weak to be detected in less sensitive observations, is required.
2. The temperature of such a component ($kT_{BB} \sim 0.8$ keV) is slightly higher than that observed with *Chandra* 3 months earlier ($kT_{BB} \sim 0.54$ keV; Woods et al. 2004).
3. Although not formally required in the fits, a blackbody component with constant temperature and luminosity is compatible with all the *XMM-Newton* observations; this requires that the variations in the source luminosity and spectrum, both on the long term and as a function of the pulsar phase, be accounted for by changes in the power-law component.
4. No absorption or emission lines are present in the 2–10 keV persistent emission with 3 σ upper limits from 30 to 100 eV on the equivalent width.
5. The 2–10 keV luminosity nearly doubled during the first half of 2004, reaching a level of $\sim 10^{36}$ ergs s^{-1}; the same trend has been observed above 20 keV with *INTEGRAL*.
6. The spectrum has been monotonically hardening during the last decade, with the power-law photon index decreasing from 2.2 to 1.5.
7. The increase in the spectral hardness and in the average spin-down rate follow, within the same source, the correlation previously found by comparing different SGRs and anomalous X-ray pulsars.
8. These changes were not accompanied by large variations in the pulse profile, even after the relatively strong sequence of bursts of 2004 October 5.
9. A blackbody with temperature of about 2 keV provides a good fit to the average burst spectra below 10 keV.
10. There is marginal evidence for an absorption feature at 4.2 keV in the burst spectra that needs to be confirmed with further data.

These findings fit reasonably well in the magnetar scenario in which the effects of a twisted magnetosphere are considered (Thompson et al. 2002). In this context we have also proposed an interpretation for the possible lines observed during the bursts.

It is clear that the hard X-ray bursting activity and the properties of the so-called persistent emission, until recently only observed below 20 keV, are strongly connected. Dramatic changes in the source properties are expected as a consequence of the enormous energy release occurred during the 2004 December 27 event. The total isotropic energy in the hard X-ray range emitted in this giant flare was of a few times 10^{46} ergs (Mazets et al. 2005; Terasawa et al. 2005; Hurley et al. 2005; Mereghetti et al. 2005b). A comparison of future X-ray observations of SGR 1806−20 with the results reported here for the "pre–giant-flare epoch" will certainly lead to a better understanding of this class of sources.

We thank N. Schartel and the staff of the *XMM-Newton* Science Operation Center for performing the 2004 October Target of Opportunity observation. This work has been partially supported by the Italian Space Agency and by the Italian Ministry for Education, University and Research (grant PRIN-2004023189). N. R. is supported by a Marie Curie Training Grant (MPMT-CT-2001-00245).

REFERENCES

Borkowski, J., Götz, D., Mereghetti, S., Mowlavi, M., Shaw, S., & Turner, M. 2004, GCN Circ. 2920, http://gcn.gsfc.nasa.gov/gcn/gcn3/2920.gcn3
Cline, T. L., et al. 1982, ApJ, 255, L45
Corbel, S., & Eikenberry, S. S. 2004, A&A, 419, 191
Duncan, R. C., & Thompson, C. 1992, ApJ, 392, L9
Fenimore, E. E., Laros, J. G., & Ulmer, A. 1994, ApJ, 432, 742
Feroci, M., Caliandro, G. A., Massaro, E., Mereghetti, S., & Woods, P. M. 2004, ApJ, 612, 408

Göğüş, E., et al. 2002, ApJ, 577, 929
Golenetskii, S. V., Aptekar, R., Mazets, E., Pal'Shin, V., Frederiks, D., & Cline, T. 2004, GCN Circ. 2769, http://gcn.gsfc.nasa.gov/gcn/gcn3/2769.gcn3
Hurley, K. 2000, in AIP Conf. Proc. 526, 5th Hunstville Symp. on Gamma-Ray Bursts, ed. R. M. Kippen, R. S. Mallozzi, & G. F. Fishman (New York: AIP), 763
Hurley, K., et al. 2005, Nature, 434, 1098
Ibrahim, A. I., Safi-Harb, S., Swank, J. H., Parke, W., Zane, S., & Turolla, R. 2002, ApJ, 574, L51
Ibrahim, A. I., Swank, J. H., & Parke, W. 2003, ApJ, 584, L17
Jones, P. B. 2003, ApJ, 595, 342
Kouveliotou, C., et al. 1998, Nature, 393, 235
Laros, J. G., Fenimore, E. E., Fikani, M. M., Klebesadel, R. W., & Barat, C. 1986, Nature, 322, 152
Lyutikov, M. 2002, ApJ, 580, L65
———. 2003, MNRAS, 346, 540
Marsden, D., & White, N. E. 2001, ApJ, 551, L155
Mazets, E. P., Golenetskii, S., Aptekar, R., Fredericks, D., Pal'Shin, V., & Cline, T. 2004, GCN Circ. 2922, http://gcn.gsfc.nasa.gov/gcn/gcn3/2922.gcn3
Mazets, E. P., et al. 1979, Nature, 282, 587
———. 2005, Nature, submitted (astro-ph/0502541)
Mereghetti, S., Chiarlone, L., Israel, G. L., & Stella, L. 2002a, MPE-Rep. 278, 29
Mereghetti, S., Cremonesi, D., Feroci, M., & Tavani, M. 2000, A&A, 361, 240
Mereghetti, S., Feroci, M., Tavani, M., & Woods, P. M. 2002b, Mem. Soc. Astron. Italiana, 73, 572
Mereghetti, S., Götz, D., Beck, M., & Mirabel, I. F. 2003, GCN Circ. 2415, http://gcn.gsfc.nasa.gov/gcn/gcn3/2415.gcn3
Mereghetti, S., Götz, D., Borkowski, J., Beck, M., & Mirabel, F. 2004, GCN Circ. 2763, http://gcn.gsfc.nasa.gov/gcn/gcn3/2763.gcn3
Mereghetti, S., Götz, D., Mirabel, I. F., & Hurley, K. 2005a, A&A, 433, L9
Mereghetti, S., Götz, D., von Kienlin, A., Rau, A., Lichti, G., Weidenspointer, G., & Jean, P. 2005b, ApJ, 624, L105
Molkov, S.V., Hurley, K., Sunyaev, R., Shtykovsky, P., Revnivtsev, M., & Kouvelioutou, C. 2005, A&A, 433, L13
Murakami, T., et al. 1994, Nature, 368, 127
Olive, J.-F., et al. 2004, ApJ, 616, 1148
Sonobe, T., et al. 1994, ApJ, 436, L23
Terasawa, T., et al. 2005, Nature, 434, 1110
Strüder, L., et al. 2001, A&A, 365, L18
Thompson, C., & Duncan, R. C. 1993, ApJ, 408, 194
———. 1995, MNRAS, 275, 255
Thompson, C., Lyutikov, M., & Kulkarni, S. R. 2002, ApJ, 574, 332
Turner, M. J. L., et al. 2001, A&A, 365, L27
Ubertini, P., et al. 2003, A&A, 411, L131
Woods, P. M., Kouveliotou, C., Göğüş E., Patel, S., Hurley, K., & Swank, J. 2004, ATel, 313, 1
Woods, P. M., & Thompson, C. 2004, preprint (astro-ph/0406133)
Woods, P. M., et al. 2000, ApJ, 535, L55
———. 2001, ApJ, 552, 748
———. 2002, ApJ, 576, 381